



X-ray properties of the starburst-driven outflow in NGC 253

I. Mitsuishi¹, N.Y. Yamasaki² and Y. Takei²

¹ Department of Physics, Tokyo Metropolitan University, 1-1 Minami-Osawa Hachioji Tokyo 192-0397 Japan, e-mail: mitsuishi@phys.se.tmu.ac.jp

² Institute of Space and Astronautical Science, Japan Aerospace Exploration Agency (ISAS/JAXA), 3-1-1 Yoshinodai, Chuo-ku Sagamihara, Kanagawa, 252-5210

Abstract. For a further understanding of a galactic-scale starburst-driven outflow, the X-ray properties of the hot interstellar gas in a well-studied nearby edge-on starburst galaxy, NGC 253, were investigated. Spectroscopic analysis was performed in three regions of the galaxy characterized by multiwavelength observations, i.e., the superwind region, the disk region and the halo region. The hot gas can be represented by two thin thermal plasmas ($kT \sim 0.2$ and ~ 0.6 keV) with various emission lines such as O, Ne, Mg, Si and Fe, in all three regions. Abundance patterns, i.e., O/Fe, Ne/Fe, Mg/Fe and Si/Fe, are consistent among the three regions, which suggests a common origin of the hot gas. Abundance patterns are heavily contaminated by type II supernova, which supports an indication that the hot gas in the halo region originates from the central starburst activity. Energetics can also provide the same conclusion if 0.01–50 $\eta^{1/2}$ % of the total emission in the nuclear region has been transported into the halo region. The obtained polytropic equation of state of the hot gas between the density and the temperature suggests that the hot gas expands adiabatically in the disk region while it moves as free expansion in the halo region towards the outer part of the halo region as the outflow. The outflow velocity of >100 km s⁻¹ is required and it is indicated that the hot gas can escape from the gravitational potential of NGC 253 by combining the outflow velocity and the thermal velocity.

Key words. starburst, X-ray, NGC 253

1. Introduction

Although metals are considered to be produced by stars in galaxies it has been known observationally that a substantial amount of metals is contained in the intergalactic medium (e.g., Songaila & Cowie 1996; Aguirre et al. 2001). However, a transport mechanism of how the metals escaped from the galaxy into an intergalactic space is still not clear and arguable.

Galactic-scale outflows can be one of solutions and starburst activity has been known to be a trigger that gives rise to the galactic-scale outflow (e.g., Strickland 2002; Heckman 2003). In a starburst-driven outflow scenario, thermal pressure due to a supernova shock associated with starburst activity pushes an ambient interstellar medium (ISM) out preferentially in the halo region which has a low-density gas. Finally, the X-ray emitting hot gas expands towards the intergalactic space as the

Send offprint requests to: I. Mitsuishi

outflow on condition that the pressure is large enough to overcome the gravitational potential of the disk and the host galaxy. To support this scenario observationally, a chemical abundance can be a good probe because α elements are provided selectively from a great deal of type II supernovae associated with the starburst activity. Abundance patterns for several starburst galaxies were reported (e.g., Yamasaki et al. 2009) and they argue that the observed ISM outside the disk originates from the inner starburst region. However, abundance patterns were not accurately constrained in some of previous studied galaxies due to poor statistics and a contamination from charge-exchange emission. Thus, abundance patterns with good quality are needed to pursue the origin of the hot gas in the halo.

NGC 253 is a nearby well-studied starburst galaxy. The edge-on orientation, its large apparent size and the wealth of multiwavelength studies allow us to discuss the spatial distribution and the outflow in detail. The distance of 3.4 Mpc (Dalcanton et al. 2009) is adopted corresponding to $16 \text{ pc arcsec}^{-1}$. All errors are at 90 % confidence level in text and tables, and at 1σ in figures.

2. Observation & data reduction

Three regions characterized by multiwavelength observations were selected to extract a continuous abundance pattern from the inner starburst region to the halo. The first one is the *superwind* region where an outflowing ionized gas is detected in the $H\alpha$ observation (Westmoquette et al. 2011) with velocity of $100\text{--}300 \text{ km s}^{-1}$ along the minor axis. The second one is the *disk* region defined as the optical disk D25 characterized by the optical B band (Pence 1980). The last one is the *halo* region characterized by a diffuse FIR emission extending up to 9 kpc perpendicular to the disk (Kaneda et al. 2009). The extracted three regions for spectral analysis are shown in Figure 1. For the *superwind* region and the *disk* region, we utilized *XMM-Newton* which has a higher angular resolution of $\sim 10''$ to remove the contamination from point sources, and good sensitivity for soft emission lines to

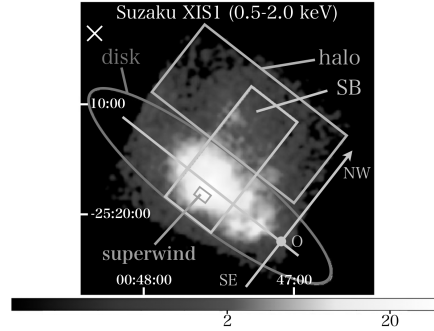


Fig. 1. *Suzaku* XIS1 image in 0.5–2 keV in the unit of $\text{cts (101 ks)}^{-1} (64 \text{ pixel})^{-1}$. Rectangles and ellipse denoted as superwind, disk and halo correspond to the extracted regions for spectral analysis. The surface brightness and the hardness ratio are extracted from the rectangle region denoted as SB. Cross mark shows the aim point of the offset region. The scale is logarithmic. Vignetting and background are not corrected for.

extract abundance patterns accurately. For the *halo* region, *Suzaku* was used because its lowest and stable background enables us to study the faint X-ray emission from the halo. To evaluate the X-ray background emission in the *halo* region, an offset region (see Figure 1) just next to NGC 253 was used.

3. Results & discussion

We extracted the spectrum in three regions and various emission lines such as O, Ne, Mg, Si and Fe were detected successfully. Spectra were fitted with an absorbed ISM and a sum of unresolved point sources. Only for the *halo* region, the X-ray background emission was estimated by simultaneous fitting with the offset observation owing to the difficulty in evaluating the X-ray background emission in the same *Suzaku* FOV. The hot gas in all three regions was represented well by two thin thermal plasmas with $kT \sim 0.2 \text{ keV}$ and $\sim 0.6 \text{ keV}$, respectively. The temperatures in the *halo* region are two times higher than those of the previous study (Bauer et al. 2008) and this discrepancy may be caused by the difference of the adopted energy band in spectral analysis. Resulting abundance patterns are con-

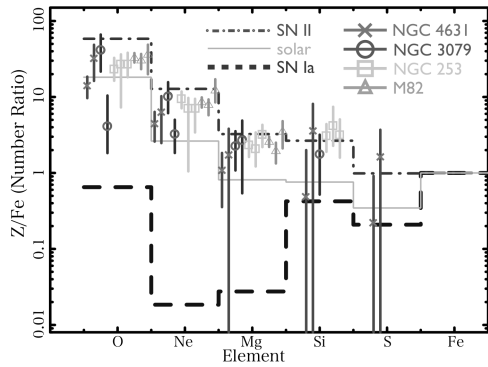


Fig. 2. Abundance patterns for starburst galaxies of NGC 4631 (cross: Yamasaki et al. 2009), NGC 3079 (circle: Konami et al. 2012), NGC 253 (rectangle: this work) and M82 (triangle: Konami et al. 2011), respectively. Dot, solid and dot-dash lines show expected products by type I supernova (Iwamoto et al. 1999), solar abundance tabulated in Anders & Grevesse (1989) as an example of solar abundance tables and type II supernova (Nomoto et al. 2006). For NGC 4631 and NGC 3079, abundance patterns in both the disk (left) and the halo (right) are plotted. Abundance patterns in the *superwind* region (left), the *disk* region (middle) and the *halo* region (right) are exhibited for NGC 253 and only in the halo are shown for M82.

sistent between the three regions, which suggests a common origin for the hot gas and consistent with those expected by type II supernova ejecta, indicating that the hot gas in the *halo* region was transported from the inner *starburst* region through the starburst activity. This result is supported by previous works on abundance patterns from other starburst galaxies, which suggest that the same chemical pollution mechanism works. Abundance patterns are summarized in Figure 2. Also from the energetics point of view, this conclusion can be explained on condition that 0.01–50 $\eta^{1/2}$ % of the total emission in the nuclear region where the most intense starburst activity occurs (e.g., Mitsuishi et al. 2011) has been transported into the *halo* region to explain the total observed luminosity and thermal energy in the *halo* region.

Next, to constrain the physical properties of the hot gas, surface brightness and hardness

ratio which can be tracers of density and temperature were investigated for the *SB* region in Figure 1. Resulting surface brightness in 0.4–0.8 keV and hardness ratio of 0.8–1.0 keV to 0.4–0.8 keV are plotted together in the NW disk and the SE disk as shown in Figure 3. As reference values, polytropic indices of 4/3, 5/3 and 6/3 assuming a simple polytropic equation of state of the hot gas ($T\rho^{1-\gamma} = \text{const}$) are also plotted. The polytropic index of 5/3 seems to be preferable for both the NW disk and the SE disk to explain the observed gradient between the surface brightness and the hardness ratio while no gradient is found in the halo, which indicates that the hot gas expands adiabatically in the disk while it moves as free expansion in the halo towards the outer part of the halo as the outflow. The surface brightness and the hardness ratio were converted to density and temperature by assuming emissivity, cylindrical emission region and an absorbed thin thermal plasma model convolved with the *Suzaku* response matrix.

Resulting density and temperature profiles are shown in Figures 4 and 5. To reproduce the observed flat temperature profile, the hot gas has to proceed at a certain level of the velocity towards the outside. Thus, we constrained the velocity of the hot gas by imposing the following three assumptions: (i) the ISM gas moves with a constant velocity in the halo, (ii) the ISM gas cools through the radiative cooling process and (iii) the density profile corresponds to that estimated from the surface brightness profile in 0.4–0.8 keV. We compared the observed temperature profile with the expected temperature profile as shown in Figure 5. The outflow velocity of 100 km s^{-1} is required to explain the observed flat temperature profile. Details are summarized in Mitsuishi et al. (2012).

Acknowledgements. I. M. is grateful to Kentaro Someya and Prof. Kazuhisa Mitsuda for useful advice of spectral analysis to extract abundance patterns and discussion to constrain the outflow velocity. Part of this work was financially supported by the Ministry of Education, Culture, Sports, Science and Technology, Grant-in Aid for Scientific Research 10J07487, 15340088 and 22111513.

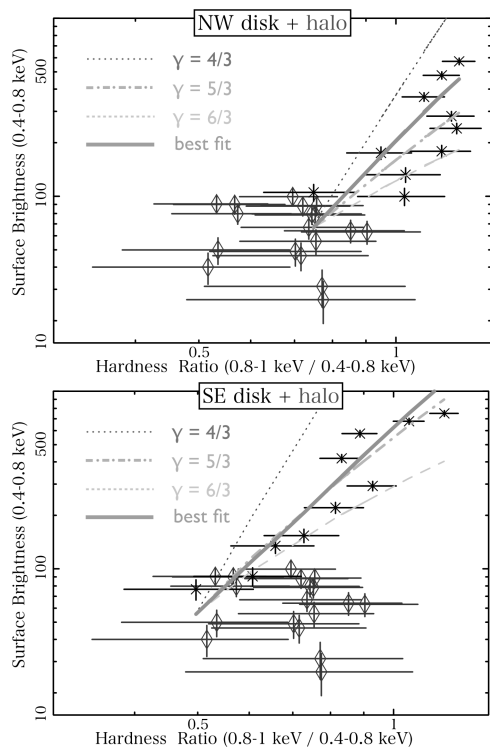


Fig. 3. Observed hardness ratio vs surface brightness for the NW disk (top) and the SE disk (bottom). Cross and diamond marks correspond to results in the disk and the halo. As reference values, polytropic indices of 6/3 (dash), 5/3 (dot-dash) and 4/3 (dot) and the best fit curves (solid) are also plotted together. The normalization of each curve is arbitrarily determined.

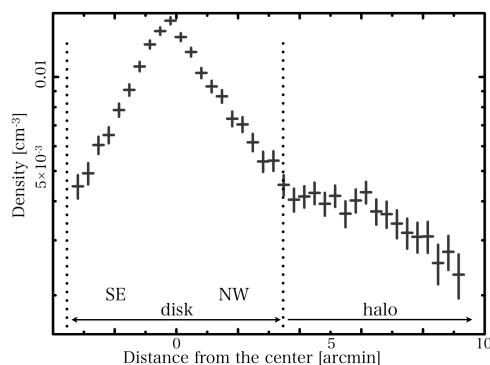


Fig. 4. Estimated density profile from the surface brightness profile in 0.4–0.8 keV.

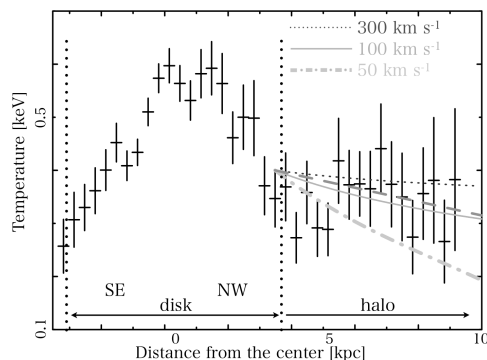


Fig. 5. Observed temperature profile obtained from the hardness ratio profile in the SB region. The expected temperature profiles with constant velocities of 300 km s^{-1} (dot), 100 km s^{-1} (solid) and 50 km s^{-1} (dot-dash) are also plotted together. Dashed line exhibits the observed steepest temperature slope within the 90% confidence level.

References

- Anders, E., & Grevesse, N., 1989, *gca*, 53, 197
 Aguirre, A., et al. 2001, *ApJ*, 560, 599
 Bauer, M., et al. 2008, *A&A*, 489, 1029
 Dalcanton, J. J., et al., 2009, *ApJS*, 183, 67
 Heckman, T. M., 2003, *Revista Mexicana de Astronomia y Astrofisica Conference Series*, 17, 47
 Iwamoto, K., et al. 1999, *ApJS*, 125, 439
 Kaneda, H., Yamagishi, M., Suzuki, T., & Onaka, T., 2009, *ApJ*, 698, L125
 Konami, S., et al. 2011, *PASJ*, 63, 913
 Konami, S., Matsushita, K., Gandhi, P., & Tamagawa, T., 2012, *PASJ*, 64, 117
 Mitsuishi, I., Yamasaki, N. Y., & Takei, Y., 2011, *ApJ*, 742, L31
 Mitsuishi, I., Yamasaki, N. Y., & Takei, Y., 2012 *PASJ*, 65, 44
 Nomoto, K., Tominaga, N., Umeda, H., Kobayashi, C., & Maeda, K., 2006, *Nuclear Physics A*, 777, 424
 Pence, W. D., 1980, *ApJ*, 239, 54
 Songaila, A., & Cowie, L. L., 1996, *AJ*, 112, 335
 Strickland, D. 2002, *Astronomical Society of the Pacific Conference Series*, 253, 387
 Westmoquette, M. S., Smith, L. J., & Gallagher, III, J. S., 2011, *MNRAS*, 414, 3719
 Yamasaki, N. Y., Sato, K., Mitsuishi, I., & Ohashi, T., 2009, *PASJ*, 61, 291